Stabilization of Luminescent Mononuclear Three-Coordinate CuI Complexes by Two Distinct Cavity-Shaped Diphosphanes Obtained from a Single α-Cyclodextrin Precursor

Tuan-Anh Phan, Matthieu Jouffroy, Dominique Matt, Nicola Armaroli, Alejandra Saavedra Moncada, Elisa Bandini, Béatrice Delavaux-Nicot, Jean-Francois Nierengarten, Dominique Armspach

Chemistry–A European Journal
Research Article
doi.org/10.1002/chem.202302750
Chemistry Europe
European Chemical Societies Publishing
www.chemeurj.org

Stabilization of Luminescent Mononuclear Three-Coordinate Cu^{I} Complexes by Two Distinct Cavity-Shaped Diphosphanes Obtained from a Single α-Cyclodextrin Precursor

Tuan-Anh Phan,[a, e] Matthieu Jouffroy,[b] Dominique Matt,[b] Nicola Armaroli,*[c] Alejandra Saavedra Moncada,[c] Elisa Bandini,[c] Béatrice Delavaux-Nicot,*[d] Jean-François Nierengarten,*[e] and Dominique Armspach*[a]

This article is dedicated to Prof. Catherine Housecroft and Prof. Edwin Constable on the occasion of their retirement

Slightly different reaction conditions afforded two distinct cavity-shaped *cis*-chelating diphosphanes from the same starting materials, namely diphenyl(2-phosphanylphenyl)phosphane and an α–cyclodextrin-derived dimesylate. Thanks to their metal-confining properties, the two diphosphanes form only mononuclear [CuX(PP)] complexes (X=Cl, Br, or I) with the tricoordinated metal ion located just above the center of the cavity. The two series of Cu^{I} complexes display markedly different luminescence properties that are both influenced by the electronic properties of the ligand and the unique steric environment provided by the cyclodextrin (CD) cavity. The excited state lifetimes of all complexes are significantly longer than those of the cavity-free analogues suggesting peculiar electronic effects that affect radiative deactivation constants. The overall picture stemming from absorption and emission data suggests close-lying charge-transfer (MLCT, XLCT) and triplet ligand-centered (LC) excited states.

Introduction

Ruthenium and iridium metal complexes are nowadays widely used as photocatalysts and photosensitizers as a result of their exceptional photophysical properties, namely strong absorption in the visible range, high reduction and oxidation potentials, as well as long-lived excited states.[1] However, the scarcity of these second row transition metals and their high toxicity have prompted chemists to look for more benign and abundant first row alternatives.[2] Among all non-noble metals, copper stands on its own since copper(I) complexes have a closed shell d^{10} ground state configuration that prevents them from exhibiting fast nonradiative deactivation of the excited state via low-lying metal-centered (MC) states as observed for other first row transition metal complexes.[3] Even if this is clearly a major asset, nonradiative deactivation processes are still present and need to be addressed for copper(I) complexes to compete with photoactive noble metal analogues. Tetracoordinated copper(I) complexes[4] are by far the most common ones, and absorption bands located in the visible part of their spectrum correspond

[a] *Dr. T.-A. Phan, Prof. D. Armspach*
Équipe Confinement Moléculaire et Catalyse
Institut de Chimie de Strasbourg, UMR 7177 CNRS
Université de Strasbourg
4 rue Blaise Pascal, CS90032
67081 Strasbourg cedex (France)
E-mail: d.armspach@unistra.fr
Homepage: http://armspach.com/

[b] *Dr. M. Jouffroy, Dr. D. Matt*
Laboratoire de Chimie Inorganique Moléculaire et Catalyse
Institut de Chimie de Strasbourg, UMR 7177 CNRS
Université de Strasbourg
4 rue Blaise Pascal, CS90032
67081 Strasbourg cedex (France)

[c] *Dr. N. Armaroli, Dr. A. S. Moncada, Dr. E. Bandini*
Istituto per la Sintesi Organica e la Fotoreattività
Consiglio Nazionale delle Ricerche
Via P. Gobetti 101, 40129 Bologna (Italy)
E-mail: nicola.armaroli@isof.cnr.it
Homepage: http://www.isof.cnr.it/armaroli_nicola/

[d] *Dr. B. Delavaux-Nicot*
Laboratoire de Chimie de Coordination du CNRS (LCC), UPR 8241
Université de Toulouse (UPS)
205 route de Narbonne, 31077 Toulouse cedex 4 (France)
E-mail: beatrice.delavaux-nicot@lcc-toulouse.fr
Homepage: http://www.lcc-toulouse.fr/dendrimeres-et-heterochimie-equipe-m/

[e] *Dr. T.-A. Phan, Dr. J.-F. Nierengarten*
Laboratoire de Chimie des Matériaux Moléculaires
Université de Strasbourg et CNRS (LIMA - UMR 7042)
Ecole Européenne de Chimie, Polymères et Matériaux
25 rue Becquerel, 67087 Strasbourg cedex 2 (France)
E-mail: nierengarten@unistra.fr
Homepage: http://nierengartengroup.com/

Supporting information for this article is available on the WWW under https://doi.org/10.1002/chem.202302750

to $d_{\pi-\pi^*}$ metal to ligand charge transfer (MLCT) transitions useful for photochemical applications. In the MLCT excited state, the copper(I) ion is formally oxidized to copper(II), while one of the ligands is reduced. This copper(II) cation undergoes a pseudo-Jahn–Teller flattening and the resulting transient state is prone to nonradiative deactivation, also via interaction with coordinating solvent molecules.[3a] On the other hand, luminescent three coordinate Cu^{I} metal complexes are relatively rare, even if some of them display remarkable photophysical properties.[3g] In particular, [CuX(PP)] (X = halide) complexes[5] in which the PP ligand is a bulky diphosphane, may display long excited state lifetimes and unusually high photoluminescence quantum yields (PLQYs) even in solution (Figure 1).[5a,b] Their highly emissive nature is a result of their 3-coordinate geometry, which lessens the effect of Jahn–Teller distortion in the excited state. However, even in these systems, nonradiative deactivation processes may still occur if a T-shaped geometry is accessible in the excited state.[6] As for tetrahedral d^{10} Cu^{I} complexes, controlling the metal coordination sphere is therefore of paramount importance for improving their photophysical properties. This can be achieved sterically by using bulky ligands, notably cavity-shaped ones that can wrap themselves around the metal center. There is a clear need for designing new macrocyclic ligands capable of imposing different steric constraints on the metal to evaluate the effect of metal encapsulation on the luminescent properties of the complexes. Recently, we have demonstrated that a cavity-shaped ligand in which a 1,2-bis(phenylphosphanyl)benzene unit is embedded in a permethylated β-CD unit, can enhance the luminescent properties of a tetrahedral $[Cu(NN)(PP)]^{+}$complex by limiting the coordination sphere distortion of the excited state.[7] In the present article, we describe two diphosphanes (**1 a** and **2**) with distinct inner-cavity environments derived from the smaller α-CD that can be elegantly synthesized from the same starting materials using slightly different reaction conditions. We then demonstrate their ability to form exclusively mononuclear trigonal [CuX(PP)] complexes by ensuring that the CuX unit (X = halide anion) remains inside the CD cavity. Finally, we provide an analysis of the electrochemical and photophysical properties of the new Cu^{I} complexes.

Results and Discussion

Diphosphane **1 a** was synthesized in a fashion similar to that for the β-CD analog **3 a**.[7] The synthesis takes advantage of a Smiles-like rearrangement of diphenyl(2-phosphanylphenyl)phosphane (**4**) in the presence of excess *n*-BuLi. The 1:1 mixture of the two resulting diastereomeric dianions **5 a,b** (Scheme 1) was reacted with α-CD-derived dimesylate **6 a** in THF to afford diphosphane-capped CDs as a 6:4 mixture consisting of, respectively, the desired confining *cis* diphosphane **1 a** (Scheme 2) and its two *trans* diastereomers **1 b,c** (Figure S2). As for the β-CD series, a single *cis* diastereomer was detected. Notably, heating the mixture of diphosphanes in boiling mesitylene (160 °C) for 4 h converted most of the unwanted *trans* diastereomers **1 b,c** into the desired *cis* diastereomer **1 a**, which obviously is sterically much more favored than the **1 b**/**1 c** pair (**1 a**/(**1 b** + **1 c**) ratio = 24). It is worth mentioning that these observations contrast with those made

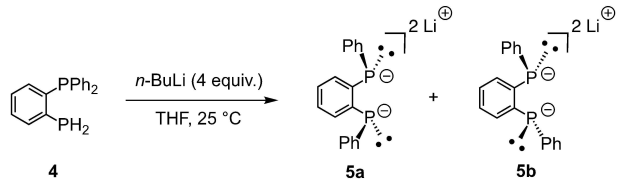

4 5a 5b

Scheme 1. Synthesis of dianions **5 a,b** from diphosphane **4** with excess *n*-BuLi.

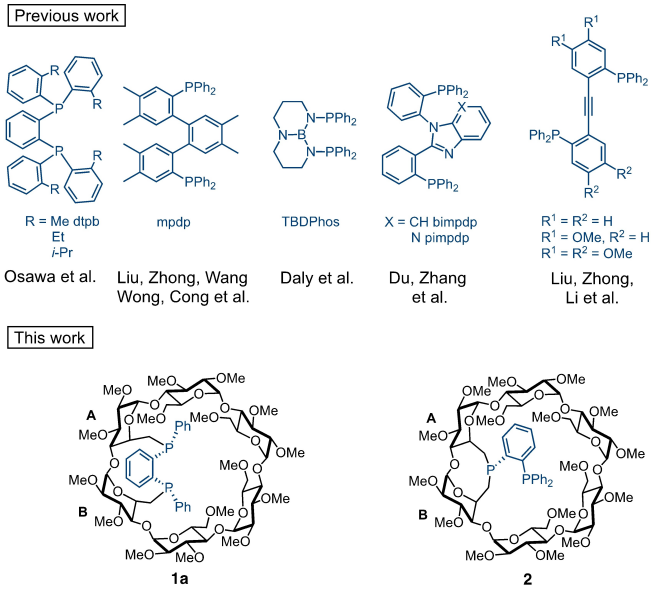

Figure 1. P,P ligands present in luminescent [CuX(PP)] complexes.

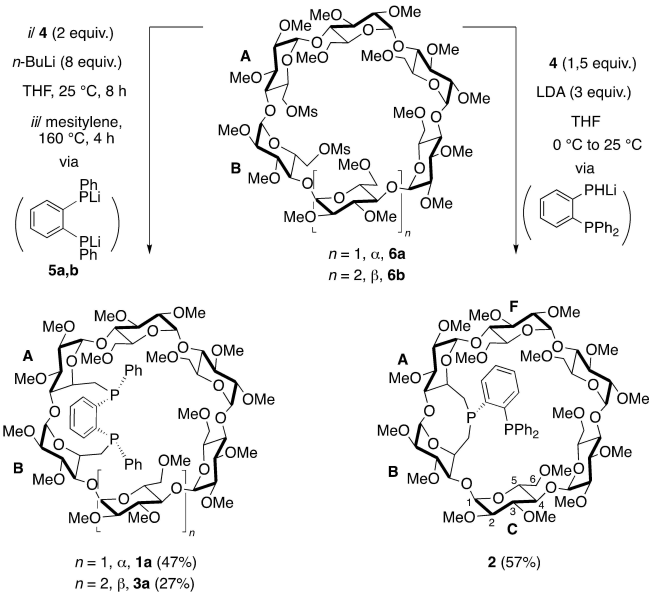

Scheme 2. Synthesis of diphosphanes **1 a, 2** and **3 a**.[9]

for the β-CD series (**3a**/(**3b**+**3c**) ratio = 1.5; **3b,c**: *trans* diastereomers of **3a**). Remarkably, the two *trans* diastereomers **1b,c** could be easily distinguished from **1a** in the ^{31}P NMR spectrum of the mixture since, for the latter, the close spatial proximity of the phosphorus lone pairs causes $^{3}J_{PP'}$ values to be rather large in the AB system ($^{3}J_{PP'}$ = 176 Hz), whereas in the formers, all phosphorus atoms resonate as singlets (Figure S2).[8] Finally, residual amounts of **1b,c** were separated from the targeted *cis* counterpart **1a** by column chromatography to afford pure **1a** in 47% yield.[9]

Pure diphosphane **2** was also synthesized from dimesylate **6a** (Scheme 2) by totally avoiding the Smiles-like rearrangement of **4**. This could be achieved by using excess lithium diisopropylamide (LDA) instead of *n*-BuLi as a base, which does not lead to the rearranged dianions **5a,b**, but instead, gives a phosphide nucleophile, most probably a monoanionic species given the lower pK_a of LDA. Such monoanion can undergo a first nucleophilic substitution with dimesylate **6a**, and the resulting CD secondary phosphane can then cyclize upon deprotonation by the remaining LDA to give the P-bridged diphosphane **2** in 57% yield (Scheme 2). Similar cyclizations have been previously performed with phenylphosphane[10] and *N*,*N*-dimethyl-2-phosphanylaniline,[11] which, unlike **4**, do not rearrange in the presence of excess *n*-BuLi. As for the latter primary phosphanes, the cyclization reaction is 100% stereoselective, the second possible diastereomer in which the phosphorus lone pair is pointing outside the cavity was not detected in the reaction mixture.

Moreover, using other strong bases for deprotonation of **4** (*t*-BuLi, PhLi, lithium bis(trimethylsilyl)amide) led to either significant amounts of rearranged products **5a,b**, even in the presence of only 2 equiv. of base or the formation of small amounts of a tetraphosphane side product (Table S1 and Figure S1). Although some of the P(III) atoms of **1a** and **2** are seemingly quite basic (δ_{31P} = −27.2 and −19 ppm for **1a** and −28.7 and −14.7 ppm for **2**), these ligands are considerably more stable against air oxidation than their PhP-bridged counterpart (δ_{31P} = −16.2 ppm) and can be purified by standard column chromatography as in the case of an analogous cavity-shaped P,N ligand without noticeable formation of phosphane oxides.[11] The presence of through-space PC couplings involving the triarylphosphane P-atom and C-6 carbon atoms of the glucose units C and F ($^{TS}J_{P,C}$ = 7.7 Hz and 3 Hz, respectively) is in agreement with a triarylphosphane unit sitting just above the CD unit (Figure S4e). These rare through-space couplings usually occur in rigid and constrained systems and reveal the close proximity between phosphorus and carbon atoms.[12]. As for **1a**, the $^{3}J_{PP'}$ coupling is rather large ($^{3}J_{PP'}$ = 167 Hz), reflecting some degree of overlap between the phosphorus lone pairs (Figure S4b). Clearly, both P donor atoms in **2** are ideally placed for chelating a metal center within the α-CD cavity. Both ligands **1a** and **2** have a cavity big enough to host a CuX unit with variable halide size. Indeed, the reaction between either **1a** or **2** with copper halides (X = chloride, bromide, or iodide) afforded respectively the mononuclear Cu^{I} complexes **7a–c** and **8a–c** in solution (Scheme 3). The DOSY diffusion coefficients of both complexes (Figures S6g and S9g) turned out to be very close to those of their respective ligands **1a** and **2** (Figures S3i, S4k), which is a clear indication of the absence of any dinuclear species comprising bridging halides[13] or tetrahedral, homoleptic $[(Cu(PP)_2]^+$ complexes[5d,14] that usually form when the metal center is not sterically protected. This result also points to a CD-encapsulated CuX unit that is prevented from interacting with a second metal center. As expected, *cis*-chelation of Cu^{I} by either diphosphane causes the PP coupling constant to increase significantly (260 Hz ≤ $J_{P,P}$ ≤ 308 Hz vs. 176 Hz and 167 Hz for ligands **1a** and **2**, respectively) and all through-space couplings to disappear. None of the inner cavity H-5 protons of either ligand undergo significant downfield shifts upon complexation. This means that the halido ligand does not interact in a significant way with inner-cavity protons in solution.[15]

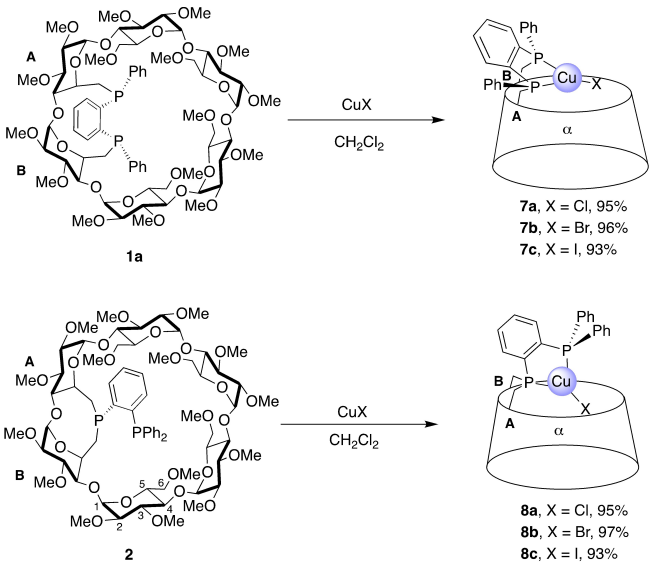

Scheme 3. Synthesis of trigonal Cu^{I} complexes **7a–c** and **8a–c** from, respectively, diphosphanes **1a** and **2**.

X-ray diffraction (XRD) studies on single crystals of **7a,b**, and **8b**[16] confirmed the presence of a chelated metal center within the α-CD cavity for both types of complexes (Figures 2 and S25-S27). All CD cavities have a familiar circular shape, with all glucose units adopting the standard $^{4}C_1$ conformation. The

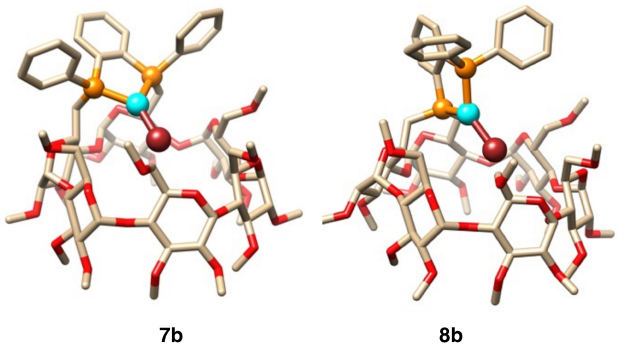

Figure 2. X-ray crystal structures of complexes **7b** and **8b** (solvent molecules and H atoms omitted for clarity; C: pale brown, O: red, P: orange, Cu: cyan, Br: dark red).

molecular structures of **7a,b** as well as that of **8b**, show a trigonal geometry with the CuX rod pointing toward the cavity interior (angle between CD O-4 atoms and the PCuXP' planes = 26.7° for **7a** and 27° for **7b**). The CuX rod of **8b** is more tilted toward the cavity interior (angle between CD O-4 atoms and the Cu–Br bond = 36.6 °) than in **7a,b**. In **7a**, one of the Cu–P bonds is significantly longer than the other (2.30 Å and 2.24 Å for **7a** vs. 2.26 Å for **7b**). This is also the case for **8b**, in which the more electron-rich phosphorus $P(alk)_2Ar$ atom forms a shorter CuP bond (2.23 Å) than the one involving the PPh_2Ar unit (2.27 Å).[17] Moreover, the PP'CuBr unit in **8b** is no longer planar as in **7a,b**, the CuBr rod forming an angle of 10.5° with the PCuP' plane. In none of the complexes, the distance between the inner-cavity H-5 protons and the halido exogenous ligand is shorter than 3 Å, in agreement with solution NMR studies which also did not reveal the presence of CH···X interactions. Finally, complexes **7a,b** display a coordination sphere very close to that of mononuclear bis(triarylphosphane) analogues described by Osawa.[5a,b]

The electrochemical properties of complexes **7a–c** and **8a–c** were studied by cyclic voltammetry (CV) and Osteryoung square wave voltammetry (OSWV). All experiments were performed at room temperature in CH_2Cl_2 solutions containing *n*-Bu_4NBF_4 (0.1 M) as supporting electrolyte, with a Pt wire as the working electrode and a saturated calomel electrode (SCE) as the reference electrode. Selected potential data for all the compounds are collected in Table 1, and the voltammograms are shown in Figures S11–S18. The oxidation potential of ligand **2** (E_{ox}^1) is close to that found for the dppb ligand (+1.04 V),[18] under our conditions, while that of the more electron-rich ligand **1a** is significantly lower (around 80 mV). Both values are close to those of triaryl-substituted phosphanes reported by Osawa,[5b] which according to their ^{31}P chemical shifts, should have similar basicity. To the best of our knowledge, electrochemical data dealing with tricoordinate [CuX(PP)] complexes are rather scarce, particularly their voltammograms, which have not been reported so far. Their electrochemical behavior is fairly complex (see Supporting Information) and very sensitive to the conditions. The OSWV voltammograms of all complexes exhibit a first major and broad oxidation process located in the 0.9–1.0 V range. A minor small oxidation process was also observed at +0.56 V and +0.72 V for **7c** and **8c**, respectively. These minor peaks are ascribed to the presence of small amounts of $[(\mathbf{1a})Cu]^+$ and $[(\mathbf{2})Cu]^+$ resulting from a dynamic coordination/decoordination of the weakly bound iodine ligand of **7c** and **8c** in solution.[19] For all the complexes, the first oxidation peak corresponds to an irreversible process and is likely metal-centered. It can be noted that the observed $Cu^{I/II}$ oxidation potentials of **7a–c** and **8a–c** are affected by the nature of the halido ligand. In both series, the E_{ox}^1 values are shifted to lower values on going from Cl to Br and from Br to I. This trend is in full agreement with the decreased electronegativity of halogens down the group 7. Further examination by cyclic voltammetry suggests that the initial Cu^I-centered oxidation is likely followed by a fast partial decomplexation process of the resulting Cu^{II} cation. The second oxidation (E_{ox}^2) is therefore ascribed to the decoordinated phosphane ligand generated upon the initial metal-centered oxidation.

The absorption spectra of ligands **1a** and **2** and the corresponding complexes **7a–c** and **8a–c** are depicted in Figure 3. Both ligands exhibit intense absorption bands in the UV region with a maximum at ~270 nm (ε = 5600–6300 M^{-1} cm^{-1} respectively), which are entirely attributed to π→π* transitions of the diphosphane units,[13,20] as α-CDs are

Table 1. Selected electrochemical data[a] of ligands **1a**, **2**, and complexes **7a–c**, **8a–c** in CH_2Cl_2 + 0.1 M *n*-Bu_4NBF_4 at room temperature.

Compound	Halido ligand	E_{ox}^{1}[b]	E_{ox}^{2}
1a		+0.96 (0.41)	
7a	Cl	+0.98 (0.43)	+1.05[c] (0.50)
7b	Br	+0.92 (0.37)	+1.06 (0.51)
7c	I	+0.90[d] (0.35)	+1.04 (0.49)
2		+1.02 (0.47)	
8a	Cl	+0.99[e] (0.44)	
8b	Br	+0.92 (0.37)	+1.09[f] (0.54)
8c	I	+0.91[g] (0.36)	+1.09 (0.54)

[a] Selected data refer to OSWV experiments; ferrocene was used as internal reference (Fc^+/Fc is observed at +0.55 ± 0.01 V vs. SCE). [b] E_{ox}^1 = first major oxidation potential expressed vs. SCE (E_{ox}^n values in brackets are expressed vs. Fc/Fc^+). [c] shoulder of E_{ox}^1 not easy to reproduce very accurately. [d] small additional oxidation process detected at +0.56 V. [e] In this case, E_{ox}^1 and E_{ox}^2 could not be distinguished. [f] Intense shoulder of the peak situated at 0.92 V. [g] minor oxidation process detected at +0.72 V.

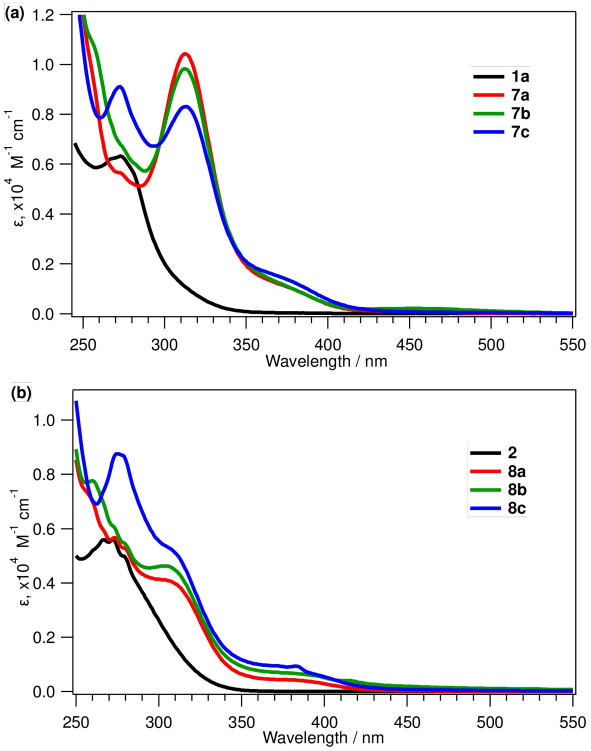

Figure 3. Absorption spectra of ligands **1a** (a) and **2** (b) and their halide complexes **7a–c** (a) and **8a–c** (b) in CH_2Cl_2.

optically transparent in the observed spectral window.[21] Among complexes **7a–c** and **8a–c**, only the iodine-containing ones (**7c** and **8c**) have a distinct feature at around 270 nm, corresponding to the maximum of the free ligand, but with higher ε values (8760–9110 M^{-1} cm^{-1} respectively). All complexes exhibit two extra absorption bands with respect to their ligands, in line with reported analogues.[5a] The first one shows a maximum in the range 306–312 nm with molar absorption coefficients for **8a–c** lower (ε = 3900–5220 M^{-1} cm^{-1}) than those of **7a–c** (ε = 8300–10400 M^{-1} cm^{-1}) and with the latter exhibiting more defined and intense features. The lowest energy band is weaker, broader, and extends up to the visible region above 400 nm. The two absorption features characteristic of the complexes are similar to those observed in trigonal Cu^{I} analogues. They can be assigned to a mixed transition (σ→π* and π→π*) and to an X→π* transition (where X is Cl, Br, or I).[5a,c,f,13,20] The absorption spectral shapes and intensities of the free ligands in CH_2Cl_2 do not vary significantly over time. On the contrary, the analogous spectra of the Cu^{I} complexes show significant changes after 24 h, especially for the **7a–c** series (Figures S19 and S20). However, these data suggest that, within 30 min after solubilization, spectroscopic measurements can be safely made.

Upon excitation at 300 nm at room temperature in CH_2Cl_2 solution, **1a** and **2** exhibit a weak emission band at ~365 nm (Figure S24). The luminescence signal of **1a** is stronger (PLQY = 0.5%) compared to that of **2** (0.1%); both exhibit a lifetime of about 35 ns, with **2** showing a longer-lived component, which is hard to attribute. The luminescence of phosphane ligands is a scarcely investigated area of research, with only scattered papers across time.[5b,22] For instance, we have reported that POP (i.e., bis[(2-diphenylphosphanyl)phenyl]ether)) exhibits luminescence at room temperature, whereas dppb (1,2-bis(diphenylphosphanyl)benzene) does not. On the other hand, they both emit at 77 K.[18] Here, the shape of the excitation spectra of **1a** and **2** (Figure S21), in comparison with the absorption profiles, suggests that the observed luminescence is genuine, despite the very weak signal in an unfavorable spectral window (240–340 nm). At 77 K, both diphosphanes show a strong phosphorescence (Figure 4b) at 520 (**1a**) and 510 nm (**2**), with excitation profiles (Figure S21) showing a neat signal at 280 nm. Excited state decays are best fitted with bi-exponential functions, dominated by the longer-lived component with a lifetime of around 350 μs. The luminescence spectra of the six Cu^{I} complexes in CH_2Cl_2 solution at 298 K have been recorded by excitation at 380 nm, in order to avoid light absorption from any traces of free ligands that might occur. The spectra are similar in shape and width (Figure 4a). However, emission bands of complexes **7a–c** are blue-shifted with respect to those of **8a–c** (Table 2), which might underpin a lower tendency to undergo T-type distortion upon light excitation.[6] This is corroborated by the fact that **2** can more easily form T-shaped [AuCl(PP)] complexes than **1a** (see below).[23] Moreover, a trend can be observed for the **7a–c** series, where the wavelength emission maximum (λ_{em}) increases in the order: **7a** > **7b** > **7c**. This behavior is in agreement with other studies, showing that the maximum λ_{em} is affected by the ligand field strength effect induced by the halogen ions in the complex ($Cl^- > Br^- > I^-$).[5a,b,13,20,24] The nature of the halide ions, which are directly bound to the copper center, notably affects the luminescent excited state. The latter has a charge transfer character, where the donor orbital can be both on the Cu center and on the halogen atom, whereas the acceptor is an antibonding orbital on the phosphane ligand (Cu→π*, MLCT; X→π*, XLCT).[5c,f] In particular, a decrease in the ligand-field strength reduces the splitting of the d-orbitals on the Cu center, leading to a larger MLCT energy and a shorter emission wavelength.[20,24d,e] The weakest ligand field occurs with the iodido ligand. Accordingly, **7c** exhibits an emission maximum at 530 nm, whereas the bands of the chloride (**7a**) and bromide analogues (**7b**) are shifted to 550 nm. In the case of the **8a–c** series, the halide ions do not significantly affect the λ_{em} of the complex, which is centered at about 600 nm. This behavior has been explained by the predominant contribution of the phosphane or halogen donor orbitals to the HOMO.[24d,25] All six Cu^{I} complexes exhibit low photoluminescence quantum yields (PLQYs) in CH_2Cl_2 solution, between 0.1 and 0.6%. Despite very low signal intensities, the excitation spectra are well-matched with the absorption profiles, corroborating the attribution.

Table 2. Photophysical data of ligands **1a** and **2** and complexes **7a–c** and **8a–c** in CH_2Cl_2 at 298 K, in frozen solution at 77 K, and in 1 wt % PMMA at 298 K.

Complex	CH_2Cl_2, 298 K			CH_2Cl_2, 77 K				PMMA (1%), K
	λ_{em} [nm]	PLQY[a] [%]	τ [ns]	λ_{em} [nm]	τ [μs][h]	λ_{em} [nm]	PLQY[e] [%]	τ [μs][h]
1a	~365[b]	0.5[b]	37[f]	~520[b]	49 (11%) 339 (89%)	~500	14.5[c]	16 (18%) 250 (82%)
7a	~550[d]	0.1[d]	38[g] (81%) 139 (19%)	~480[d]	492	~528	7.5[d]	247
7b	~550[d]	0.1[d]	40[g] (13%) 514 (87%)	~470[d]	122 (51%) 369 (49%)	~500	6.8[d]	17 (15%) 275 (85%)
7c	~530[d]	0.3[d]	30[g] (31%) 196 (69%)	~490[d]	26 (34%) 293 (66%)	~480	5.1[d]	11 (53%) 252 (47%)
2	~365[b]	0.1[b]	33[f] (24%) 302 (76%)	~510[b]	48 (9%) 359 (91%)	~500	2.2[c]	216
8a	~600[d]	0.6[d]	46[g] (5%) 221 (95%)	~488[d]	501	~535	4.5[d]	65 (14%) 350 (86%)
8b	~600[d]	0.4[d]	62[g] (8%) 232 (92%)	~485[d]	135 (58%) 259 (42%)	~545	1.0[d]	20 (7%) 260 (93%)
8c	~600[d]	0.4[d]	63[g] (11%) 215 (89%)	~480[d]	39 (47%) 343 (53%)	~495	5.2[d]	241

[a] Measured with respect to $[Ru(bpy)_3]^{2+}$ as standard (PLQY = 0.028 in air equilibrated water); [b] λ_{exc} = 300 nm; [c] λ_{exc} = 320 nm; [d] λ_{exc} = 380 nm; [e] Determined using an integrating sphere; [f] λ_{exc} = 331 nm NanoLED; [g] λ_{exc} = 373 nm NanoLED; [h] λ_{exc} = 370 nm SpectraLED.

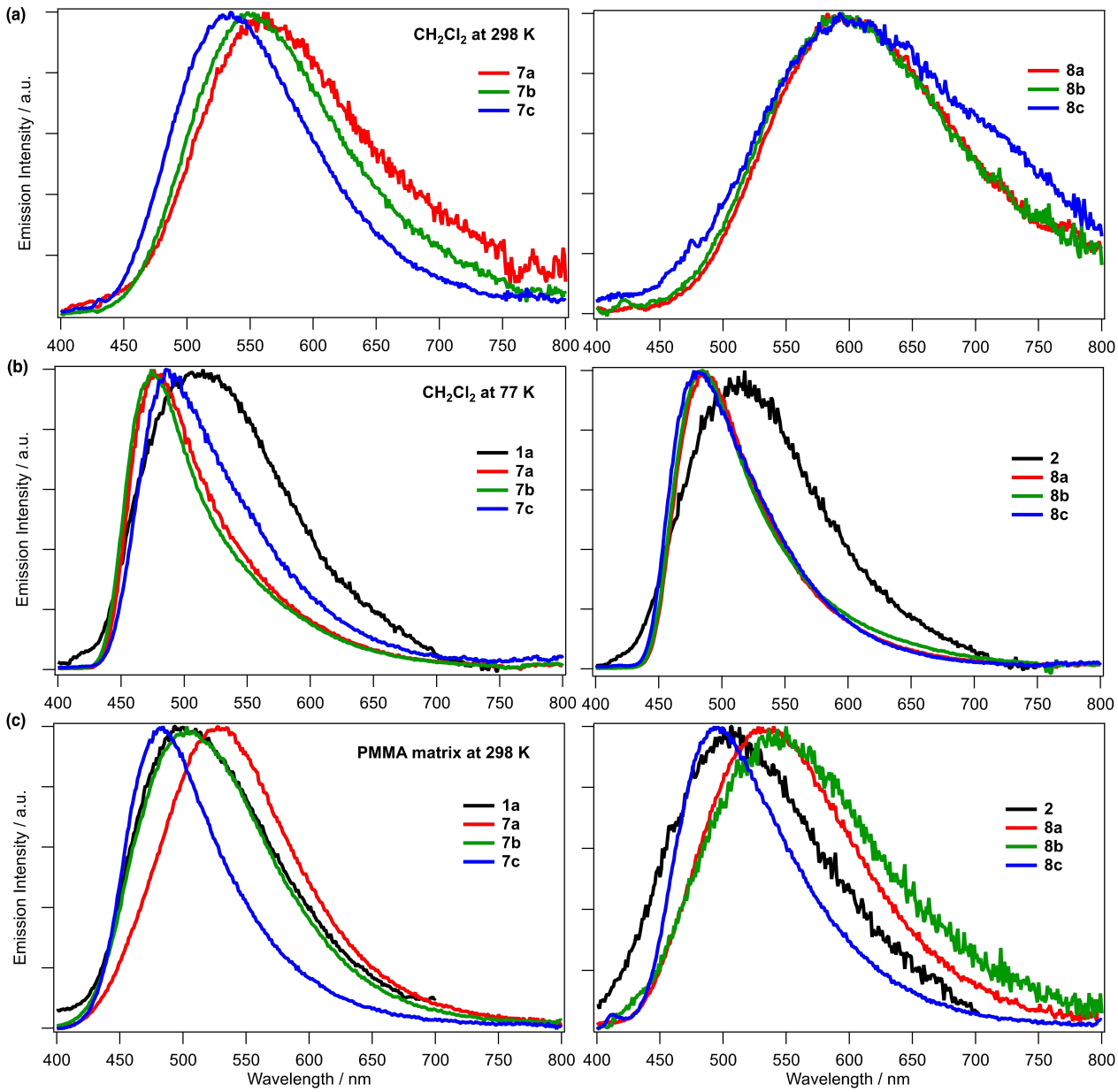

Figure 4. Emission spectra of ligand **1a** and complexes **7a–c** (column left), and ligand **2** and complexes **8a–c** (column right) in (a) CH_2Cl_2 at 298 K, $\lambda_{ex}=380$ nm; (b) in CH_2Cl_2 at 77 K, $\lambda_{ex}=300$ nm for ligands and $\lambda_{ex}=380$ nm for complexes; (c) in PMMA 1 wt% at 298 K, $\lambda_{ex}=320$ nm for ligands and $\lambda_{ex}=380$ nm for complexes.

In rigid CH_2Cl_2 matrix at 77 K (Figure 4b), the emission bands of the six complexes are more intense and remarkably blue-shifted with respect to 298 K, i.e., by about 120 nm for the **8a–c** series ($\lambda_{em}=$~480 nm), and 70 nm for the **7a–c** one ($\lambda_{em}=$470–490 nm). This behavior has been observed previously in Cu^{I} complexes[26] and highlights the predominance of rigidochromic effects in the glass matrix on electronic effects. The excited state lifetimes (also measured by exciting outside the free ligand absorption window) are generally biexponential, as it often happens with Cu^{I} complexes with phosphane ligands.[5f,26b] At 298 K, the longer component (in the range 220–230 ns) is largely predominant for **8a–8c**. For **7a–7c**, the situation is more complicated with the shorter component nearly identical for all compounds (30–40 ns) and the longer one rather scattered. 77 K lifetimes are much longer. The two chloride complexes **7a** and **8a** exhibit mono-exponential decays around 500 μs. In contrast, the two iodine and bromine-based systems show bi-exponential decays with similar contributions, made of a longer component in the range ca. 260–370 μs and a shorter lifetime, which, in the case of the iodido complexes is as short as 26 (**7c**) and 39 μs (**8c**). In the related bromide complexes (**7b** and **8b**), such a component is substantially longer (122 and 135 μs).

The luminescence properties were also investigated in PMMA matrix at 298 K (Figure 4c), and the emission intensity is significantly stronger than in CH_2Cl_2 solution at 298 K. The **7a–c** complexes exhibit more intense emissions (PLQYs = 5–7%) than

their **8a–c** counterparts (PLQYs = 1–5%), most likely because T-type distortion upon light excitation is facilitated in **8a–c** as revealed by the X-ray crystal structure of the [AuCl(**2**)] gold(I) analog of **8a** which is clearly more T-shaped than complex [AuCl(**1a**)] in the solid state.[23] The **7a–c** series also displays the same blue spectral shift observed in CH_2Cl_2 at 77 K, with λ_{em} increasing in the following order: **7a** > **7b** > **7c** ($Cl^- > Br^- > I^-$). This trend can be rationalized by ligand field arguments, as suggested above. However, such a trend is not observed for **8a–c**, even if the two iodido complexes are the most blue-shifted and exhibit similar PLQYs at around 5%. This behavior can be ascribed to the relatively weaker ligand field and larger atomic number of the iodide ion.[24e]

Compared to analogous cavity-free trigonal [CuX(PP)] complexes studied by Osawa et al.,[5a,b] Daly et al.,[5d] and Du, Zhang et al.,[5f] the PLQYs of the systems presented here are significantly lower, whether in solution or in the solid state, and more in line with those observed by Liu, Zhong, Wang, Wong, Cong et al.[5c] On the other hand, the excited state lifetimes in amorphous films at room temperature of all of our Cu^I complexes are about two-orders of magnitude longer than those observed by Osawa.[5a] This result might indicate a different nature of the excited state of the present system compared to Osawa's, also considering the rather different radiative constant ($k_r = \Phi/\tau$) observed for **7a** in solution ($7.2\times10^3\ s^{-1}$), compared to Osawa's Cu^I chlorido analog ($8.8\times10^4\ s^{-1}$)[5a] which comprises the dtpb = 1,2-bis(*o*-ditolylphosphanyl)benzene] ligand. It cannot be ruled out that the luminescence bands of the metal complexes presented here are - at least partially - attributable to ligand-centered (LC) triplet excited states. As a matter of fact, the onset of the 77 K phosphorescence spectra of **7a** and **8** at around 400 nm is well matched with the end of the charge-transfer absorption bands of the metal complexes. Therefore LC, MLCT and XLCT excited states are expected to be very close in energy, which makes the interpretation of the photophysical behavior particularly challenging. The complex pattern of experimental data is compelling in PMMA rigid matrix, where the emission spectrum of the ligand **1a** is fully overlapped with the bromide complex **7b**, whereas the chloride and iodide systems (**7a**, **7c**) – despite virtually identical onsets - have a substantially different spectral width and/or shape. Another interesting difference between our cavity-shaped complexes and Osawa's systems is that the former have emission maxima that tend to be red-shifted by up to 80 nm in fluid solution, and this effect is particularly marked in the case of the **8a–c** series.

The intricate picture that emerged in the present study is prompting us to deepen our investigation and carry out extensive DFT and TD-DFT studies to clarify the complex pattern of the photophysical results, also in relation to (*i*) the likely interplay between charge-transfer states and ligand centered triplets; (*ii*) the properties observed for the bare phosphane ligands, to be further investigated; (*iii*) the need to clarify any influence of the appended CD cage. Other d^{10} metal ions are also being considered in order to get an even deeper insight into the electronic and excited state properties of this intriguing family of trigonal complexes.

Conclusions

By avoiding the previously described Smiles-like rearrangement using the weaker base LDA for the deprotonation of diphenyl(2-phosphanylphenyl)phosphane and subsequent cyclization with the α-CD-based dimesylate **6**, access to a new type of *cis*-chelating diphosphane (**2**) with metal-confining properties was made possible. When using the stronger *n*-BuLi base instead of LDA, the smaller α-CD analog (**1a**) of previously reported diphosphane **3a** was obtained with excellent stereoselectivity. Both diphosphanes, which display somewhat different electronic properties, are able to force a single chelated metal center to reside inside the CD cavity but with a distinct steric environment around the metal. The two types of trigonal [CuX(PP)] complexes obtained give rise to different photophysical properties, but both with unusually long-lived excited states. Theoretical studies are currently in progress to rationalize these differences and have a complete elucidation of the ground and excited state properties of these intriguing classes of metal complexes that incorporate a simple trigonal coordination motif within a complex, cage-like architecture. The ability of these new cavity-shaped, *cis*-chelating P,P ligands to promote the exclusive formation of mononuclear complexes showing metal encapsulation is also currently exploited for catalytic purposes,[27] notably in ethylene oligomerization.[11]

Experimental Section

Procedure for the synthesis of diphosphane **1a**. A solution of *n*-BuLi in hexane (1.6 M, 2.77 mL, 4.33 mmol) was added dropwise to a stirred solution of **4** (0.326 g, 1.11 mmol) in thf (16 mL) at −78 °C. After 10 min, the reaction mixture was allowed to reach room temperature and then kept at this temperature for 8 h under stirring. The resulting red suspension was cannulated within 15 min into a stirred solution of dimesylate **6a** (0.75 g, 0.55 mmol) in thf (45 mL). The reaction mixture was stirred for 12 h at room temperature. The solvent was then removed *in vacuo* and excess $(LiPPh)_2Ar$ was protonated with MeOH (5 mL). After removal of the solvent *in vacuo*, mesitylene (20 mL) was added and the resulting solution was heated at reflux for 4 h. Removal of the solvent *in vacuo*, afforded a colorless solid, which was filtered over a short plug of silica using CH_2Cl_2/MeOH (500 mL, 90:10, *v*/*v*) as solvent. The resulting colorless residue was then subjected to column chromatography (SiO_2, CH_2Cl_2/MeOH, 97:3, *v*/*v*) to afford **1a** (yield: 0.38 g, 47%) as a colorless solid.

Procedure for the synthesis of diphosphane **2**. A solution of LDA in thf/heptane/ethyl benzene (2.0 M, 1.11 mL, 2.22 mmol) was added dropwise to a stirred solution of **4** (0.262 g, 0.89 mmol) in thf (10 mL) at −78 °C. The red solution was stirred at −78 °C for 10 min before being allowed to reach 0 °C over 20 min. The resulting red suspension maintained at 0 °C was cannulated within 5 min into a stirred solution of dimesylate **6a** (1.00 g, 0.74 mmol) in thf (24 mL) at 0 °C. The reaction mixture was stirred for 12 h at room temperature. The solvent was then removed *in vacuo* and excess $LiPHArPPh_2$ was protonated with MeOH (5 mL). Removal of the solvent *in vacuo*, afforded a colorless solid, which was filtered over a short plug of silica using CH_2Cl_2/MeOH (500 mL, 90:10, *v*/*v*) as solvent. After removal of the solvent *in vacuo*, the resulting colorless residue was subjected to column chromatography (SiO_2,

CH_2Cl_2/MeOH, 97:3, *v/v*) to afford **2** (yield: 0.61 g, 57%) as a colorless solid.

General procedure for the synthesis of complexes **7a–c** and **8a–c** Anhydrous CuX (X = Cl, Br or I) (0.06 mmol) was added to a solution of **1a** or **2** (0.06 mmol) in CH_2Cl_2 (3 mL) under stirring. After 2 h, the reaction mixture was filtered over Celite® and the filtrate was evaporated under vacuum. The resulting solid was washed with pentane to afford the corresponding [CuX(PP)] complex (93–97%) as a pale yellow solid.

Supporting Information

Detailed experimental materials and methods as well as supplementary figures and tables, experimental spectra and X-ray crystallographic data are available in the Supporting Information. The authors have cited additional references within the Supporting Information.[28]

Acknowledgements

This work was supported by the CNR through the CNR-CNRS joint lab D10-GREEN "d^{10} Metal Architectures for Green Lighting, Photoredox Catalysis and Remote Sensing" and the Interdisciplinary Thematic Institute SysChem, via the IdEx Unistra (ANR 10-IDEX-0002) within the French Investments for the Future Program. T.-A.P. further thanks the *Fondation Jean-Marie Lehn* (University of Strasbourg – Frontier Research in Chemistry) for his PhD fellowship. We also thank Dr. A. Sournia-Saquet (LCC) for electrochemical measurements.

Conflict of Interests

The authors declare no conflict of interest.

Data Availability Statement

The data that support the findings of this study are available from the corresponding authors, upon reasonable request.

Keywords: copper · cyclodextrin · halide · luminescence · phosphane

[1] a) Y. Chi, P. T. Chou, *Chem. Soc. Rev.* **2010**, *39*, 638–655; b) V. W. W. Yam, K. M. C. Wong, *Chem. Commun.* **2011**, *47*, 11579–11592; c) Q. A. Zhao, F. Y. Li, C. H. Huang, *Chem. Soc. Rev.* **2010**, *39*, 3007–3030; d) C. K. Prier, D. A. Rankic, D. W. C. MacMillan, *Chem. Rev.* **2013**, *113*, 5322–5363.
[2] C. Bizzarri, E. Spuling, D. M. Knoll, D. Volz, S. Bräse, *Coord. Chem. Rev.* **2018**, *373*, 49–82.
[3] a) N. Armaroli, G. Accorsi, F. Cardinali, A. Listorti, *Top. Curr. Chem.* **2007**, *280*, 69–115; b) A. Lavie-Cambot, M. Cantuel, Y. Leydet, G. Jonusauskas, D. M. Bassani, N. D. McClenaghan, *Coord. Chem. Rev.* **2008**, *252*, 2572–2584; c) S. Paria, O. Reiser, *ChemCatChem* **2014**, *6*, 2477–2483; d) M. J. Leitl, D. M. Zink, A. Schinabeck, T. Baumann, D. Volz, H. Yersin, *Top. Curr. Chem.* **2016**, *374(25)*; e) O. Reiser, *Acc. Chem. Res.* **2016**, *49*, 1990–1996; f) T. P. Nicholls, A. C. Bissember, *Tetrahedron Lett.* **2019**, *60*, 150883; g) J. Beaudelot, S. Oger, S. Perusko, T. A. Phan, T. Teunens, C. Moucheron, G. Evano, *Chem. Rev.* **2022**, *122*, 16365–16609; h) H. Takeda, A. Kobayashi, K. Tsuge, *Coord. Chem. Rev.* **2022**, *470*, 214700.
[4] Y. M. Zhang, M. Schulz, M. Wächtler, M. Karnahl, B. Dietzek, *Coord. Chem. Rev.* **2018**, *356*, 127–146.
[5] a) M. Hashimoto, S. Igawa, M. Yashima, I. Kawata, M. Hoshino, M. Osawa, *J. Am. Chem. Soc.* **2011**, *133*, 10348–10351; b) M. Osawa, M. Hoshino, M. Hashimoto, I. Kawata, S. Igawa, M. Yashima, *Dalton Trans.* **2015**, *44*, 8369–8378; c) L. P. Liu, R. Zhang, L. Liu, X. X. Zhong, F. B. Li, L. Wang, W. Y. Wong, G. H. Li, H. J. Cong, N. S. Alharbi, Y. Zhao, *New. J. Chem.* **2019**, *43*, 3390–3399; d) K. Lee, P. N. Lai, R. Parveen, C. M. Donahue, M. M. Wymore, B. A. Massman, B. Vlaisavljevich, T. S. Teets, S. R. Daly, *Chem. Commun.* **2020**, *56*, 9110–9113; e) X. Y. Dong, Z. L. Li, Q. S. Gu, X. Y. Liu, *J. Am. Chem. Soc.* **2022**, *144*, 17319–17329; f) S. Liu, J. Y. Zhang, C. M. Liu, G. J. Yin, M. Wu, C. X. Du, B. Zhang, *Polyhedron* **2022**, *218*, 115761; g) N. A. Liu, L. Liu, X. X. Zhong, F. B. Li, F. Y. Li, H. M. Qin, *New. J. Chem.* **2022**, *46*, 3236–3247.
[6] T. Y. Li, D. S. M. Ravinson, R. Haiges, P. I. Djurovich, M. E. Thompson, *J. Am. Chem. Soc.* **2020**, *142*, 6158–6172.
[7] T. A. Phan, N. Armaroli, A. S. Moncada, E. Bandini, B. Delavaux-Nicot, J. F. Nierengarten, D. Armspach, *Angew. Chem. Int. Ed.* **2023**, *62*, e202214638.
[8] P. B. Hitchcock, M. F. Lappert, W. P. Leung, P. Yin, *J. Chem. Soc., Dalton Trans.* **1995**, 3925–3932.
[9] Unlike **1a**, two additional metallation/demetallation steps (see Ref. [7]) are required to access pure **3a**.
[10] a) E. Engeldinger, L. Poorters, D. Armspach, D. Matt, L. Toupet, *Chem. Commun.* **2004**, 634–635; b) R. Gramage-Doria, D. Rodriguez-Lucena, D. Armspach, C. Egloff, M. Jouffroy, D. Matt, L. Toupet, *Chem. Eur. J.* **2011**, *17*, 3911–3921.
[11] Y. Li, K. Pelzer, D. Sechet, G. Creste, D. Matt, P. Braunstein, D. Armspach, *Dalton Trans.* **2022**, *51*, 11226–11230.
[12] a) L. Poorters, D. Armspach, D. Matt, L. Toupet, S. Choua, P. Turek, *Chem. Eur. J.* **2007**, *13*, 9448–9461; b) J. C. Hierso, D. Armspach, D. Matt, *C. R. Chim.* **2009**, *12*, 1002–1013.
[13] A. Tsuboyama, K. Kuge, M. Furugori, S. Okada, M. Hoshino, K. Ueno, *Inorg. Chem.* **2007**, *46*, 1992–2001.
[14] a) P. C. Healy, J. C. McMurtrie, J. Bouzaid, *Acta Crystallogr. E* **2010**, *66*, M493-U271; b) K. Saito, S. Saijo, K. Kotera, T. Date, *Chem. Pharm. Bull.* **1985**, *33*, 1342–1350.
[15] E. Engeldinger, D. Armspach, D. Matt, P. G. Jones, R. Welter, *Angew. Chem. Int. Ed.* **2002**, *41*, 2593–2596.
[16] Deposition Number's 2280885 (for **7a**), 2280887 (for **7b**) 2280888 (for **8b**) contain the supplementary crystallographic data for this paper. These data are provided free of charge by the joint Cambridge Crystallographic Data Centre and Fachinformationszentrum Karlsruhe Access Structures service.
[17] Distances and angles are averaged values calculated from the two slightly different structures present in the asymmetric units.
[18] A. Kaeser, O. Moudam, G. Accorsi, I. Seguy, J. Navarro, A. Belbakra, C. Duhayon, N. Armaroli, B. Delavaux-Nicot, J. F. Nierengarten, *Eur. J. Inorg. Chem.* **2014**, *2014*, 1345–1355.
[19] A. Poirot, C. Vanucci-Bacque, B. Delavaux-Nicot, N. Saffon-Merceron, C. L. Serpentini, N. Leygue, F. Bedos-Belval, E. Benoist, S. Fery-Forgues, *Photochem. Photobio. Sci.* **2023**, *22*, 169–184.
[20] X. Hong, B. Wang, L. Liu, X. X. Zhong, F. B. Li, L. Wang, W. Y. Wong, H. M. Qin, Y. H. Lo, *J. Lumin.* **2016**, *180*, 64–72.
[21] G. Benkovics, M. Malanga, E. Fenyvesi, *Int. J. Pharm.* **2017**, *531*, 689–700.
[22] D. J. Fife, W. M. Moore, K. W. Morse, *Inorg. Chem.* **1984**, *23*, 1545–1549.
[23] Unpublished results.
[24] a) M. J. Leitl, F. R. Kuchle, H. A. Mayer, L. Wesemann, H. Yersin, *J. Phys. Chem. A* **2013**, *117*, 11823–11836; b) D. M. Zink, M. Bächle, T. Baumann, M. Nieger, M. Kuhn, C. Wang, W. Klopper, U. Monkowius, T. Hofbeck, H. Yersin, S. Bräse, *Inorg. Chem.* **2013**, *52*, 2292–2305; c) L. J. Kang, J. Chen, T. Teng, X. L. Chen, R. M. Yu, C. Z. Lu, *Dalton Trans.* **2015**, *44*, 11649–11659; d) S. K. Gibbons, R. P. Hughes, D. S. Glueck, A. T. Royappa, A. L. Rheingold, R. B. Arthur, A. D. Nicholas, H. H. Patterson, *Inorg. Chem.* **2017**, *56*, 12809–12820; e) J. H. Jia, X. L. Chen, J. Z. Liao, D. Liang, M. X. Yang, R. M. Yu, C. Z. Lu, *Dalton Trans.* **2019**, *48*, 1418–1426.
[25] K. Tsuge, Y. Chishina, H. Hashiguchi, Y. Sasaki, M. Kato, S. Ishizaka, N. Kitamura, *Coord. Chem. Rev.* **2016**, *306*, 636–651.
[26] a) M. Mohankumar, M. Holler, E. Meichsner, J.-F. Nierengarten, F. Niess, J.-P. Sauvage, B. Delavaux-Nicot, E. Leoni, F. Monti, J. M. Malicka, M. Cocchi, E. Bandini, N. Armaroli, *J. Am. Chem. Soc.* **2018**, *140*, 2336–2347; b) E. Leoni, J. Mohanraj, M. Holler, M. Mohankumar, I. Nierengarten, F. Monti, A. Sournia-Saquet, B. Delavaux-Nicot, J. F. Nierengarten, N.

Armaroli, *Inorg. Chem.* **2018**, *57*, 15537–15549; c) J. J. Cid, J. Mohanraj, M. Mohankumar, M. Holler, F. Monti, G. Accorsi, L. Karmazin-Brelot, I. Nierengarten, J. M. Malicka, M. Cocchi, B. Delavaux-Nicot, N. Armaroli, J. F. Nierengarten, *Polyhedron* **2014**, *82*, 158–172.

[27] a) M. Jouffroy, D. Armspach, D. Matt, *Dalton Trans.* **2015**, *44*, 12942–12969; b) Z. Kaya, E. Bentouhami, K. Pelzer, D. Armspach, *Coord. Chem. Rev.* **2021**, *445*, 214066.

[28] a) D. Armspach, L. Poorters, D. Matt, B. Benmerad, F. Balegroune, L. Toupet, *Org. Biomol. Chem.* **2005**, *3*, 2588–2592; b) S. Basra, J. G. de Vries, D. J. Hyett, G. Harrison, K. M. Heslop, A. G. Orpen, P. G. Pringle, K. von der Luehe, *Dalton Trans.* **2004**, 1901–1905; c) G. A. Crosby, J. N. Demas, *J. Phys. Chem.* **1971**, *75*, 991–1024; d) K. Nakamaru, *Bull. Chem. Soc. Jpn.* **1982**, *55*, 2697–2705; e) C. Würth, M. Grabolle, J. Pauli, M. Spieles, U. Resch-Genger, *Nat. Protoc.* **2013**, *8*, 1535–1550.

Manuscript received: August 22, 2023
Accepted manuscript online: November 23, 2023
Version of record online: December 18, 2023